



**Characteristics of the  
raindrop distributions  
in RICO shallow  
cumulus**

O. Geoffroy et al.

**Characteristics of the raindrop  
distributions in RICO shallow cumulus**

O. Geoffroy<sup>1</sup>, A. P. Siebesma<sup>2</sup>, and F. Burnet<sup>1</sup>

<sup>1</sup>CNRM-GAME, Toulouse, France

<sup>2</sup>KNMI, De Bilt, Holland

Received: 22 November 2013 – Accepted: 18 December 2013 – Published: 9 January 2014

Correspondence to: O. Geoffroy (olivier.geoffroy@meteo.fr)

Published by Copernicus Publications on behalf of the European Geosciences Union.

Title Page

Abstract

Introduction

Conclusions

References

Tables

Figures



Back

Close

Full Screen / Esc

Printer-friendly Version

Interactive Discussion





## Characteristics of the raindrop distributions in RICO shallow cumulus

O. Geoffroy et al.

Title Page

Abstract

Introduction

Conclusions

References

Tables

Figures

⏪

⏩

◀

▶

Back

Close

Full Screen / Esc

Printer-friendly Version

Interactive Discussion

hand, large drop formation is limited by two microphysical processes: collision-induced breakup and spontaneous breakup. The latter occurs for diameters of a value of the order of about 10 mm (Pruppacher and Pitter, 1971). Both breakup processes contribute to a broadening of the raindrop distribution. The effect of collision-coalescence-breakup processes leads to an equilibrium distribution in around one hour (Hu and Srivastava, 1995), which corresponds to about twice the lifetime of a boundary layer cloud cell. In unsaturated regions, the raindrop spectra evolve as the result of evaporation. In addition to these processes, the sedimentation process redistributes the rain drop sizes in the vertical: because large drops fall faster, raindrops are sorted by size (Milbrandt and Yau, 2005; Seifert, 2008). Thus, assuming a continuous and steady production of rain at cloud top, the rain distribution at a given level is in equilibrium only if the lifetime of the precipitating event is large enough to counteract the sedimentation size sorting effect. Ultimately, local raindrop distribution is the result of a coupling between advection, turbulent transport and microphysical processes; i.e., collision-coalescence-breakup and sedimentation in clouds in a first stage, and evaporation, sedimentation and to a lower extent collision-coalescence-breakup out of the cloud in a second stage.

Under some hypotheses, each microphysical main variable and process can be written as functions of the integral variables of the rain distribution, mostly moments. The moment of the order  $p$   $M_p$  is defined following:

$$M_p = \int_0^{\infty} D^p n(D) dD \quad (1)$$

where  $D$  is the particle diameter and  $n(D)$  is the probability distribution of raindrop size. The raindrop number concentration  $N_r$  is the 0th moment of the distribution. The rainwater content  $q_r$  is proportional to the 3rd moment of the distribution. Both are prognostic variables in two-moment bulk schemes. The 6th moment of the distribution is called the radar reflectivity factor and is proportional to the radar reflectivity, which is a useful quantity for remote sensing measurements. The collection of cloud droplets by raindrops (accretion) depends on the product of cloud and rain water contents (Kessler,

## Characteristics of the raindrop distributions in RICO shallow cumulus

O. Geoffroy et al.

Title Page

Abstract

Introduction

Conclusions

References

Tables

Figures

⏪

⏩

◀

▶

Back

Close

Full Screen / Esc

Printer-friendly Version

Interactive Discussion

1969). The raindrop terminal velocity is roughly proportional to the diameter to the power 0.8. Thus the sedimentation fluxes of the rain concentration and the rainwater content vary as a linear function of the moments 0.8 and 3.8, respectively; i.e., they are roughly dependent on  $M_1$  and  $M_4$ . The evaporation rate is the sum of two linear functions depending roughly on the moments of the order 0.8 and 1.8.

Since only a limited number of rainfall integral variables are generally known (e.g.  $M_0$  and  $M_3$  in 2-moment bulk schemes,  $M_6$  in remote sensing measurement), a hypothesis on the shape of the distribution is necessary in order to derive the other microphysical properties. Raindrop distributions are generally represented by the exponential law (Marshall and Palmer, 1949), hereafter referred to as MP distribution, or by a gamma distribution function (Ulbricht, 1983). The latter is expressed as

$$n(D) = N \frac{1}{\Gamma(\nu)} \lambda^\nu D^{\nu-1} \exp(-\lambda D) \quad (2)$$

It has 3 independent parameters: the number concentration  $N$ , the slope parameter  $\lambda$  and the shape parameter  $\nu$ . The Gamma law is a general case of the exponential function ( $\nu = 1$ ). Note that the most common expression used for the shape parameter is  $\mu = \nu - 1$  rather than  $\nu$ . The latter is used in this study because it is defined on  $]0, +\infty[$ , which permits plots on the logarithmic scale. The slope parameter  $\lambda$  is related to the mean volume diameter  $D_v$  and  $\nu$  following:

$$\lambda = \left( \frac{1}{D_v} \nu(\nu + 1)(\nu + 2) \right)^{1/3} \quad (3)$$

In some studies the Lognormal distribution is assessed (Feingold and Levin, 1986):

$$n(D) = N \frac{1}{\sqrt{2\pi} D \ln \sigma_g} \exp \left( -\frac{1}{2} \left( \frac{\ln(D/D_g)}{\ln \sigma_g} \right)^2 \right) \quad (4)$$

where  $\sigma_g$  is the geometric standard deviation and  $D_g$  is the mean geometric diameter.

## Characteristics of the raindrop distributions in RICO shallow cumulus

O. Geoffroy et al.

Title Page

Abstract

Introduction

Conclusions

References

Tables

Figures

⏪

⏩

◀

▶

Back

Close

Full Screen / Esc

Printer-friendly Version

Interactive Discussion



The benefit of using these distributions is that each moment of the distribution can be analytically calculated as a function of the 3 parameters. In a 2-moment bulk scheme, 2 parameters are imposed by the prognostic variables and one remains to be fixed:  $\nu$  for the Gamma and  $\sigma_g$  for the Lognormal distribution. Figure 1 shows the moments of the order 1, 2, 4 and 6 as a function of the shape parameters for fixed concentration ( $M_0$ ) and water content ( $M_3$ ). When  $\nu$  increases, the distribution is narrower; i.e.,  $M_p$  increases with  $\nu$  for  $p < 3$  and decreases for  $p > 3$  and inversely for the Lognormal law. For  $\nu > 10$  or  $\sigma_g < 1.1$ , each moment does not vary significantly because the distribution tends to the monodispersed distribution. Note that, in this study, narrow (broad) refers to spectra with high (low) value of  $\nu$  or low (high) value of  $\sigma_g$  and not to high standard deviation values, which also depend on the mean volume diameter.

Since the work of Marshall and Palmer (1949) and Best (1950), a large number of studies have been dedicated to the retrieval of the value of these parameters characteristic of deep convective events. Most of these studies suggest that rain spectra are narrower than the MP distribution ( $\nu = 1$ ), with  $\nu$  values roughly in the range 5–10 (Nzeukou et al., 2003; Uijlenhoet et al., 2003) or more (Tokay and Short, 1996) or  $\sigma_g$  values of the order of 1.4 (Feingold and Levin, 1986). These studies are based on one-minute surface measurements with the RD-69 disdrometer (Joss and Waldvogel, 1967). Ulbrich and Atlas (1997) airborne 2-D precipitation probe measurements at 6 s-resolution suggest broader spectra, with a mean value of 5 ( $\mu = \nu - 1 = 6$ ), than the Tokay and Short (1996) mean value of 11, for the same field experiment. By analyzing one-minute resolution spectra derived from video disdrometer measurements at the surface, Brandes et al. (2003) also find broad spectra, with most values falling between the MP value and  $\nu = 5$ . Van Zanten et al. (2005) find narrow drizzle spectra in stratocumulus despite the coarse resolution of 2 min, with  $\sigma_g$  values of the order of 1.5–1.8.

Studies diverge not only in the shape parameter values but also in their relationship with other variables. Experimental studies show a positive correlation between  $\nu$  and the precipitation flux (Tokay and Short, 1996; Cerro et al., 1997; Nzeukou et al., 2004)



lations. Moreover, the use of complete distributions allows analytical integrations. For these reasons, this study is limited to complete functions. Moreover, such truncations do not significantly modify the results. The following section describes the data set and gives an insight into the vertical profiles of the measured precipitation fields; the shape parameters analysis results are reported in Sect. 3.

## 2 Data set and vertical structure of the precipitation field

The spectra used in this study are derived from in situ shallow precipitating cumulus cloud measurements taken during the RICO field experiment (Rauber et al., 2007; Snodgrass, 2008; Nuijens et al., 2009). Two instruments are combined to obtain the raindrop spectra used in that study. The PMS-OAP-260-X allows drizzle to be measured in a range from  $5\ \mu\text{m}$  to  $635\ \mu\text{m}$  over 63 bins of  $10\ \mu\text{m}$ . The PMS-2DP measures the diameters of larger drops over 32 to 64 bins of  $200\ \mu\text{m}$  between  $100\ \mu\text{m}$  and an upper limit depending on the method used by the NCAR to construct the particle spectra from the PMS-2DP images.

The Entire-in method takes into account only particles that fully cross the sampling section and assumes that the diameter is the drop height. The sampling volume decreases with drop diameter because the upper limit of the measured diameter is restricted by the height of the diodes, which is of the order of 6 mm. The Center-in method also takes into account partially sampled drops by accounting for all particles for which the center is within the sampling section, assuming that the diameter value is the maximum value between the depth and the height of the drop. This method increases the 2DP sampling volume and allows larger drops, up to  $12\ 700\ \mu\text{m}$ , to be taken into account.

Large rain drop diameters are especially subject to be biased due to their non spherical shape (Pruppacher and Beard, 1970; Chandrasekar et al., 1988), their low statistical representation and spurious counts (Heymsfield and Baumgardner, 1985; Backer

### Characteristics of the raindrop distributions in RICO shallow cumulus

O. Geoffroy et al.

Title Page

Abstract

Introduction

Conclusions

References

Tables

Figures



Back

Close

Full Screen / Esc

Printer-friendly Version

Interactive Discussion



et al., 2009). Thus, the Center-in spectra are used in this study and sensitivity tests are performed according to the method used in Sect. 3.

The sampled volume is of the order of 1–4 L and 100–200 L respectively for the PMS-OAP-260X and the PMS-2DP at 1 Hz resolution. This is low compared to the order of magnitude of raindrop concentration, which is about  $0.1\text{--}100\text{ L}^{-1}$ . This statistical representation problem could be partly solved by decreasing resolution. However, because of the spatial heterogeneity of the raindrops, the broadness of the spectra is sensitive to the resolution.

Spurious counts, which affect both low and high diameters (Backer et al., 2009), are removed in 2DP and OAP-260-X measurements. Similarly to Yuter and Houze (1997), all non-consecutive bins above  $1500\text{ }\mu\text{m}$  are set to 0, and the single positive bin in OAP-260-X are excluded. Because the moments of the distribution are sensitive to the extremities of the distribution, sensitivity tests to the extremities of the distribution are performed in Sect. 3.

The lower limit of the rain drop spectra  $D_0$ , which corresponds to the separation diameter with the cloud droplet category, is assumed to be  $75\text{ }\mu\text{m}$ . The results presented here are not sensitive to the chosen  $D_0$  value, at least in the range  $50\text{--}100\text{ }\mu\text{m}$ . The PMS-2DP bins are added by excluding the first one in order to avoid overlap with the OAP-260-X measurements. Thus, the measured spectra are continuous spectra covering the entire range of sizes of precipitating drops from  $D_0$  to  $12\text{ mm}$ .

Of the nineteen RICO flights analyzed in this study, thirteen are characterized by significant rainy events (RF01, RF03, RF04, RF05, RF07, RF08, RF10, RF11, RF13, RF14, RF15, RF16, RF19) and six are rejected due to the insignificant number of rain samples (RF02, RF06, RF09, RF12, RF17, RF18). Rain spectra are defined as spectra where  $q_r > 0.010\text{ gm}^{-3}$ . The total number of precipitating samples at 1 Hz resolution is of the order of 21 000. During RICO, the NCAR C-130 aircraft flew through the cloud field at different altitudes between about 100 m and 3 km. The first two plots of Fig. 2 show the number of rain spectra sampled at each level of the boundary layer in cloud

## Characteristics of the raindrop distributions in RICO shallow cumulus

O. Geoffroy et al.

Title Page

Abstract

Introduction

Conclusions

References

Tables

Figures



Back

Close

Full Screen / Esc

Printer-friendly Version

Interactive Discussion

region and in clear sky. Because the plane was pointing towards the cloud cells, a large part of the rain spectra (almost 60 %) is in cloud samples.

The vertical structure of the main rain variables is represented in Fig. 2 for the thirteen cases studied. For flights where the Fast FSSP measurements are available (blue symbols), profiles are averaged in cloud (left column) and clear sky profile (middle column). The third plot of Fig. 2 shows the vertical profile of the cloud water content. The following plots show the profiles of the rain concentration  $N_r$ , the rain concentration flux  $F_{Nr}$ , the rain water content rain precipitation flux  $F_{qr}$  and the mean volume diameter  $D_v$ . Values are averaged over the rain fraction at the corresponding level. Hence, these profiles are not directly comparable to a mean profile over the whole domain or over the projected cloud fraction. Above the cloud base, some rain falls in clear sky. This feature may be due to the shear, to turbulent motions, or to the fact that raindrops have a longer lifespan than cloud droplets. Such a pattern was seen in the Dutch atmospheric model DALES LES simulations of shallow cumulus even without shear (not shown). However, in LES simulations, a large part of the rain mass is in clear sky, which is not suggested by  $q_r$  and  $F_{qr}$  profiles. As expected, all quantities are larger in clouds due to evaporation in clear sky.

The profiles of  $q_r$  and  $F_{qr}$  do not show a particular trend with altitude. While evaporation leads to a decrease of these quantities in the subcloud layer, here values are averaged over the rain fraction, which decreases with height, compensating for the effects of evaporation. Moreover, the lack of a clear trend may be the result of a lack of horizontal and vertical statistical representation. On the other hand, the rain number concentration  $N_r$  (and the rain concentration flux) and the mean volume diameter  $D_v$  decrease and increase with decreasing altitude, respectively. All processes (collection, evaporation, sedimentation) contribute to a decrease of the number concentration and of the rain concentration flux (collection, evaporation, sedimentation), which explains the clear trends. As for the mean volume diameter, the superposition of evaporation on the size sorting effect results in a decrease of small drops with decreasing altitude and thus an increase of the mean volume diameter. The average values are similar for the

## Characteristics of the raindrop distributions in RICO shallow cumulus

O. Geoffroy et al.

Title Page

Abstract

Introduction

Conclusions

References

Tables

Figures



Back

Close

Full Screen / Esc

Printer-friendly Version

Interactive Discussion

four cloud systems. The trends shown here are similar to those observed in stratocumulus clouds (Wood et al., 2005), except that the rain concentration and the volume diameter also vary above the cloud condensation level, both in and outside the cloud.

Some studies have examined the relationship between the slope parameter  $\lambda$  and the shape parameter  $\nu$  in the aim of remote sensing retrieval of rain distribution characteristics, mainly the precipitation flux, from radar measurements (Zhang et al., 2001; Chang et al., 2009). Atlas and Ulbricht (2006) suggest that there is no universal relationship that would describe all types of storm spectra accurately. The RICO measurements confirm this fact because of the large range of mean volume diameters covered and its dependency on altitude. Assuming that the Gamma distribution gives an accurate representation of the rain spectra,  $\lambda$  depends on  $\nu$  and  $D_v$  (Eq. 3). Because the profile of  $D_v$  varies significantly with height, it follows that the  $\lambda - \nu$  relationship depends necessarily on the altitude.

This study is restricted to the estimation of the shape parameter of both Lognormal and Gamma laws assuming that  $N_r$  and  $q_r$  are known, as is the case in a simulation using a 2-moment bulk microphysics scheme. Figure 3 shows the space parameter of  $N_r$  and  $q_r$  for all RICO spectra at 1 Hz resolution. The rainwater content and the concentration cover a large range of values typical of drizzle and of more intense precipitating events. Some samples have high local rainwater content between 1 and 10  $\text{g m}^{-2}$ . Some spectra concentrations are typical of drizzle: about 50 % of the sample values are greater than 5  $\text{L}^{-1}$  and 10 % greater than 50  $\text{L}^{-1}$ . The mean volume diameter ranges from 100  $\mu\text{m}$  to about 1 mm near the surface. The RICO spectra have a lower diameter and lower concentration than those observed in deep convection. Considering the large range of values covered, it seems reasonable to assume that all kinds of rain spectra typical of shallow cumulus are statistically represented.

## Characteristics of the raindrop distributions in RICO shallow cumulus

O. Geoffroy et al.

Title Page

Abstract

Introduction

Conclusions

References

Tables

Figures

⏪

⏩

◀

▶

Back

Close

Full Screen / Esc

Printer-friendly Version

Interactive Discussion

### 3 Shape parameters analysis results

In this section, the validity of the Lognormal and the Gamma distributions in representing shallow cumulus spectra is evaluated. Figure 4 shows the shape parameters for each moment ( $M_1$ ,  $M_2$ ,  $M_4$  and  $M_6$ ) estimation as a function of the considered moment. The number of samples in each moment class is represented in the last row. The value of  $\nu$  is represented on a log-scale because of the strong dependence of moments with  $\log(\nu)$  (Fig. 1). The circles and triangles are the shape parameter values that minimize, in each moment class, the arithmetic and the geometric standard deviation of the absolute and relative errors, respectively.

For each minimization, there is a strong scatter in the  $\nu$  estimation, ranging roughly from 1 to 10. The  $M_6$  minimization gives narrower spectra on average, especially for the Lognormal model, because of the highest dissymmetry of this function. However, high order moments are sensitive to the presence of large drops. When spurious counts are not cleaned, broader spectra are obtained for the  $M_6$  minimization. Despite the large scatter observed in the shape parameters and the dependence of the results on the chosen moment, data are merged together in order to derive a trade-off value of the shape parameters and to determine a single law representative of all processes.

The trade-off values  $\nu^*$  and  $\sigma_g^*$ , of the Gamma and the Lognormal law, respectively, are calculated by averaging the 80 optimum shape parameter values in each bin following G10 for the different resolutions 1, 0.5, 0.2, and 0.05 Hz (i.e., a distance of the order of 100, 200, 500 and 2000 m, respectively). The results are summarized in Table 1.

A value of 3.2 for  $\nu^*$  and 1.63 for  $\sigma_g^*$  is obtained from the cleaned spectra (noted E2). The broadness of the spectra increases with resolution, as expected, because of the high heterogeneity of the rain field. At the scale of the cloud cell, distributions are close to the MP distribution ( $\nu = 1$ ). Table 1 also shows the arithmetic and geometrical means of each ensemble of shape parameter values. The geometric mean of the Gamma law shape parameter  $\nu$  and the arithmetic mean of the Lognormal law shape parameter  $\sigma_g$  are close to the trade-off values  $\nu^*$  and  $\sigma_g^*$ , respectively. These results suggest that

such methods of averaging (geometric mean for the Gamma and arithmetic mean for the Lognormal) are adequate for estimating the shape parameter. Moreover, this is consistent with the logarithmic and linear dependency of the moments for the Gamma and the Lognormal laws, respectively. The arithmetic mean, generally used in studies to retrieve the characteristic  $\nu$  value of the rain distributions, has significantly higher values.

To gain insight into the errors associated with the spurious count for both large and small drops and those associated with a lack of statistical representation, sensitivity tests to the tail of the rain spectra were performed. Without removing the spurious count, the Entire-in method (E) and Center-in method (C) give similar results, which suggest a low contribution of the drops larger than 6 mm, with a  $\nu^*$  value of the order of 2. This value should give a lower boundary for  $\nu^*$ . Truncations under 300  $\mu\text{m}$  in diameter (i.e. use of only 2DP measurements), above 1.5 mm and both show that the shape parameter value is mostly sensitive to the presence of the smallest drops. Spectra obtained are narrower, with an extreme value of  $\nu^*$  equal to 9 at 1 Hz, which should give a comfortable estimation of its upper bound. Such truncated spectra are close to the Joss and Waldvogel (1967) disdrometer range. The 0.05 Hz value of  $\nu^*$  is close to that derived from most previous studies.

Most studies that suggest narrow distributions are based on ground measurements. RICO measurements show an increase of  $\nu$  with decreasing altitude (Fig. 5d). This is consistent with experimental studies that show narrower distributions at the surface than in clouds for the same case study (Tokay and Short, 1996; Ulbrich and Atlas, 1998) and with 1-D numerical studies focusing on the effect of size sorting (Milbrandt and Yau, 2005; Seifert, 2008).

For spectra sampled at comparable spatial and horizontal resolutions, the shape parameters retrieved in this study differ from those reported in previous studies focusing on deep convective events. These discrepancies are due to differences in rain characteristics specific to the cloud regime (lower mean volume diameters and larger rain number concentrations in shallow cumulus), but not exclusively. They can also be

## Characteristics of the raindrop distributions in RICO shallow cumulus

O. Geoffroy et al.

Title Page

Abstract

Introduction

Conclusions

References

Tables

Figures



Back

Close

Full Screen / Esc

Printer-friendly Version

Interactive Discussion

partially attributed to instrumental limits, averaging procedures and the location of the samples.

As in G10, ACE-2 stratocumulus case measurements were also analyzed. However, they have not been included in the present study because the ACE-2 particle counter upper boundary is not high enough (350  $\mu\text{m}$ ) to cover a reasonable range of raindrop diameters: the last bin is often non zero. However, assuming this upper truncation has no significant impact, the results obtained by analyzing ACE-2 data set are in agreement with RICO spectra typical of drizzle (Fig. 5a–c), i.e. with  $\sigma_g^*$  values of the order of 1.5 and  $\nu^*$  values of the order of 5. Moreover, these values are quantitatively consistent with van Zanten et al. (2005) DYCOMS-II stratocumulus two-minute averaged spectra. As a second step, the sensitivity of the shape parameters to variables prognosticated in 2-moment bulk schemes,  $q_r$ ,  $N_r$  and thus  $D_v$ , was examined (Fig. 5a–c). The largest scatter in the 6th box plot of Fig. 5b corresponds to the transition between the OAP-200-X and the 2DP measurements marked by an important decrease in resolution (from 10 to 200  $\mu\text{m}$ ). Measurements show a clear negative trend as a function of  $q_r$ . As for  $N_r$  and  $D_v$ , no trend is observed over the whole range they cover. High concentrations and intermediate mean volume diameters are characterized by the broadest spectra but with a large spread. For low concentrations and low and high diameters, the distributions are narrow, consistent with Seifert (2008) and Milbrandt and Yau (2005).

At the early stage of their evolution (low  $D_v$ ), spectra are narrow. For intermediate values of the mean volume diameter and high rainwater content, broadness increases. Distribution tends to be narrower near the surface, where the mean volume diameter increases and the concentration decreases, due to size sorting.

Because samples are mainly in clouds or close to clouds, trade-off values derived in this study may be more representative of the first stages of rain development and not typical of subcloud layer rain spectra. However, because these large drops reach the ground and are not subject to complete evaporation, it may be more important to represent distribution in the upper levels in order to represent raindrop growth and evaporation accurately. If raindrops are size-sorted during their fall and spectra narrower

## Characteristics of the raindrop distributions in RICO shallow cumulus

O. Geoffroy et al.

Title Page

Abstract

Introduction

Conclusions

References

Tables

Figures

⏪

⏩

◀

▶

Back

Close

Full Screen / Esc

Printer-friendly Version

Interactive Discussion

## Characteristics of the raindrop distributions in RICO shallow cumulus

O. Geoffroy et al.

Title Page

Abstract

Introduction

Conclusions

References

Tables

Figures

⏪

⏩

◀

▶

Back

Close

Full Screen / Esc

Printer-friendly Version

Interactive Discussion

than predicted, it will lead to an overestimation of the fall velocity. However, evaporation of a large raindrop is low because its lifetime in the subsaturated air is short. A 2 mm drop falling in an 80 % relative humidity environment covers a distance of 2 km in 4 min and loses about 3 % of its mass. In comparison, a 200  $\mu\text{m}$  drop in the same conditions evaporates completely after 11 min and after a distance of about 700 m. Thus, the predicted amount of rain that evaporates and the amount of precipitation that reaches the ground would not be considerably biased.

As for cloud droplet spectra (G10), the shape parameter is mostly sensitive to the water content. In order to take into account size sorting and avoid a possible bias in remaining spurious counts, the shape parameter is parameterized as a function of a power law of  $q_r$  and also  $N_r$ . Figure 4 a, b shows scatterplots of  $\nu$  and  $\sigma_g$  as a function of  $N_r q_r^{0.25}$  and  $N_r q_r^{0.1}$ , respectively, for the 4 moments and the values that minimize both absolute and relative errors in each bin.

For each law, the resulting 80 optimum parameters are fitted which leads to the following expressions:

$$\begin{aligned} \nu^p &= 18 / (N_r q_r)^{0.25}, \\ \sigma_g^p &= 1. + 0.30 \cdot (N_r q_r)^{0.1} \end{aligned} \quad (6)$$

where  $q_r$  is expressed in  $\text{gm}^{-3}$  and  $N_r$  in  $\text{m}^{-3}$ .

In order to compare the accuracy of each analytical distribution to represent the rain spectra, relative and absolute errors between measured and theoretical moments are calculated. Table 2 summarizes the offsets and standard deviations of the absolute and relative errors over the whole range of moment values calculated for the gamma and the Lognormal distribution, with trade-off and parameterized values. Both laws give similar results. The parameterized expressions improve the results in terms of both bias and standard deviation.

## 4 Conclusions

RICO in situ measurements of rain spectra were analyzed in order to validate the common analytical representation of raindrop spectra and quantify the broadness of these distributions for shallow cumulus clouds. Two combined data sets from two instruments, the PMS-OAP-260-X and the PMS-2DP, were used in order to cover the full range of raindrop sizes for shallow cumulus clouds. Aircraft measurements make it possible to cover a large panel of raindrop spectra typical of this type of cloud by flying at different levels in the boundary layer. First, the profiles of the microphysical rain variables were described. Some profiles show the clear signature of microphysical processes. The rain number concentration and the mean volume diameter decrease and increase with decreasing altitude, respectively.

Next, the broadness of the distribution was studied via the relationship between a considered moment of the distribution and the two main rain variables used in microphysical schemes: the rain mixing ratio and the rain number concentration. All moments of the distribution representative of a physical process were considered separately. For a given spectra, there is generally not a single value of the shape parameter that accurately represents each moment simultaneously. Nevertheless, a constant trade-off value is proposed for both the Gamma law and the Lognormal law. On the ensemble, spectra are found to be broad at the scale of an LES model, with trade-off values  $\nu^*$  of the order of 3.2 and  $\sigma_g^*$  of the order of 1.63. At a coarser scale, distributions tend to be broader, with values of the shape parameter close to the MP value, which reflects the heterogeneity of the raindrop field. Considering differences in the location of the samples, as well as instruments, these results are consistent with studies of the literature focusing on deep convective events. Sensitivity tests to the extreme values of the distribution suggest that the contribution of the smallest drops to the broadness of the distribution is important. The Lognormal and the Gamma laws give similar results. However, the Gamma law allows analytical integration – for instance, the integration of sedimentation flux using Roger et al. (1993) parameterization of the terminal velocity.

## Characteristics of the raindrop distributions in RICO shallow cumulus

O. Geoffroy et al.

Title Page

Abstract

Introduction

Conclusions

References

Tables

Figures

⏪

⏩

◀

▶

Back

Close

Full Screen / Esc

Printer-friendly Version

Interactive Discussion

As a second step, dependency as a function of the prognostic variables of a LES microphysical scheme was explored. The best dependency is found to be with the rainwater content, and a parameterization in function of a power law of  $q_r N_r$  that improves the representation of the rain spectra was developed for the LES scale. The shape parameter's dependence on the rain variable is consistent with the effect of the microphysical processes. Spectra are narrow at the early stage of their evolution (low  $D_v$ ). Then they broaden as rain becomes more intense. Finally, the rain spectra tend to be narrower near the surface due to size sorting. This behavior may be taken into account in a LES model. However, tests with a LES model suggest that the use of the tradeoff value is sufficient to represent the magnitude of precipitation in shallow cumulus clouds. Questions remain for deep convection. Moreover, the measurements of raindrop spectra are limited by the low statistical representation of raindrops and by instrumental biases. These measurements are important for reconstructing rain history in the boundary layer and subsequently for constraining rain formation – the main source of uncertainty in precipitation calculation – at the scale of the cloud system. The results presented here highlight the importance of improving and performing particle measurements over the whole spectrum range and at all stages of rain development, i.e. in the whole boundary layer.

*Acknowledgements.* We gratefully thank J.-L. Brenguier for helpful discussions and comments on the work. O. Thouron, A. Seifert and B. Stevens are also thanked for discussions on this topic.

## References

- Baker, B., Mo, Q., Lawson, R. P., O'Connor, D., and Korolev, A.: Drop size distributions and the lack of small drops in RICO rain shafts, *J. Appl. Meteorol. Clim.*, 48, 616–623, 2009.
- Best, A. C.: The size distribution of raindrops, *Q. J. Roy. Meteor. Soc.*, 76, 16–36, 1950.
- Brandes, E. A., Zhang, G., and Vivekanandan, J.: An evaluation of a drop distribution-based polarimetric radar rainfall estimator, *J. Appl. Meteorol.*, 42, 652–660, 2003.

## Characteristics of the raindrop distributions in RICO shallow cumulus

O. Geoffroy et al.

Title Page

Abstract

Introduction

Conclusions

References

Tables

Figures

⏪

⏩

◀

▶

Back

Close

Full Screen / Esc

Printer-friendly Version

Interactive Discussion

- Cerro, C., Codina, B., Bech, J., and Lorente, J.: Modeling raindrop size distribution and Z(R) relations in the Western Mediterranean Area, *J. Appl. Meteorol.*, 36, 1470–1479, 1997.
- Chandrasekar, V., Cooper, W. A., and Bringi, V. N.: Axis ratios and oscillations of raindrops, *J. Atmos. Sci.*, 45, 1323–1333, 1988.
- 5 Chang, W. Y., Chen Wang, T. C., and Lin, P. L.: Characteristics of the raindrop size distribution and drop shape relation in typhoon systems in the Western Pacific from the 2-D video disdrometer and NCU C-Band Polarimetric Radar, *J. Atmos. Ocean. Tech.*, 26, 10, 1973–1993, 2009
- Feingold, G. and Levin, Z.: The lognormal fit to raindrop spectra from frontal convective clouds in Israel, *J. Clim. Appl. Meteorol.*, 25, 1346–1363, 1986.
- 10 Geoffroy, O., Brenguier, J.-L., and Burnet, F.: Parametric representation of the cloud droplet spectra for LES warm bulk microphysical schemes, *Atmos. Chem. Phys.*, 10, 4835–4848, doi:10.5194/acp-10-4835-2010, 2010.
- Heus, T., van Heerwaarden, C. C., Jonker, H. J. J., Pier Siebesma, A., Axelsen, S., van den Dries, K., Geoffroy, O., Moene, A. F., Pino, D., de Roode, S. R., and Vilà-Guerau de Arellano, J.: Formulation of the Dutch Atmospheric Large-Eddy Simulation (DALES) and overview of its applications, *Geosci. Model Dev.*, 3, 415–444, doi:10.5194/gmd-3-415-2010, 2010.
- 15 Heymsfield, A. J. and Baumgardner, D.: Summary of a workshop on processing 2-D probe data, *B. Am. Meteorol. Soc.*, 66, 437–440, 1985.
- Hu, Z. and Srivastava, R. C.: Evolution of raindrop size distribution by coalescence, breakup, and evaporation: theory and observations, *J. Atmos. Sci.*, 52, 1761–1783, 1995.
- Joss, J. and Waldvogel, A.: Raindrop size distribution and sampling size errors, *J. Atmos. Sci.*, 26, 566–569, 1969.
- 25 Kessler, E.: On the distribution and continuity of water substance in atmospheric circulation, *Meteor. Mon.*, 32, 1–84, 1969.
- Marshall, J. S. and Palmer, W.: The distribution of raindrops with size, *J. Meteorol.*, 5, 165–166, 1948.
- Milbrandt, J. and Yau, M.: A multimoment bulk microphysics parameterization – Part 1: Analysis of the role of the spectral shape parameter, *J. Atmos. Sci.*, 62, 3051–3064, 2005.
- 30 Nuijens, L., Stevens, B., and Siebesma, A. P.: The environment of precipitating shallow cumulus convection, *J. Atmos. Sci.*, 66, 1962–1979, 2009.

- Nzeukou, A., Sauvageot, H., Ochou, A. D., and Kebe, C. M. F.: Raindrop size distribution and radar parameters at Cape Verde, *J. Appl. Meteorol.*, 43, 90–105, 2004.
- Pruppacher, H. R. and Beard, K. V.: A wind tunnel investigation of the internal circulation and shape of water drops falling at terminal velocity in air, *Q. J. Roy. Meteor. Soc.*, 96, 247–256, 1970.
- Pruppacher, H. R. and Pitter, R. L.: A semi-empirical determination of the shape of cloud and raindrops, *J. Atmos. Sci.*, 28, 86–94, 1971.
- Rauber, R. M., Ochs III, H. T., Di Girolamo, L., Göke, S., Snodgrass, E., Stevens, B., Knight, C., Jensen, J. B., Lenschow, D. H., Rilling, R. A., Rogers, D. C., Stith, J. L., Albrecht, B. A., Zuidema, P., Blyth, A. M., Fairall, C. W., Brewer, W. A., Tucker, S., Lasher-Trapp, S. G., Mayol-Bracero, O. L., Vali, G., Geerts, B., Anderson, J. R., Baker, B. A., Lawson, R. P., Bandy, A. R., Thornton, D. C., Burnet, E., Brenguier, J.-L., Gomes, L., Brown, P. R. A., Chuang, P., Cotton, W. R., Gerber, H., Heikes, B. G., Hudson, J. G., Kollias, P., Krueger, S. K., Nuijens, L., O’Sullivan, D. W., Siebesma, A. P., and Twohy, C. H.: Rain in (shallow) cumulus over the ocean – the RICO campaign, *B. Am. Meteorol. Soc.*, 88, 1912–1928, 2007.
- Rogers, R. R., Baumgardner, D., Ethier, S. A., Carter, D. A., and Ecklund, W. L.: Comparison of raindrop size distributions measured by radar wind profiler and by airplane, *J. Appl. Meteorol.*, 32, 694–699, 1993.
- Seifert, A.: On the parameterization of evaporation of raindrops as simulated by a one-dimensional rainshaft model, *J. Atmos. Sci.*, 65, 3608–3619, 2008.
- Seifert, A. and Beheng, K. D.: A double-moment parameterization for simulating autoconversion, accretion, and self-collection, *Atmos. Res.*, 59–60, 265–281, 2001.
- Snodgrass, E. R., Girolamo, L. D., and Rauber, R. M.: Precipitation characteristics of trade wind clouds during RICO derived from radar, satellite, and aircraft measurements, *J. Appl. Meteorol.*, 48, 464–483, 2009.
- Stevens, B. and Seifert, A.: Understanding macrophysical outcomes of microphysical choices in simulations of shallow cumulus convection, *J. Meteorol. Soc. Jpn.*, 86, 143–162, 2008.
- Tokay, A. and Short, D. A.: Evidence from tropical raindrop spectra of the origin of rain from stratiform and convective clouds, *J. Appl. Meteorol.*, 35, 355–371, 1996.
- Uijlenhoet, R., Steiner, M., and Smith, J. A.: Variability of raindrop size distributions in a squall line and implications for radar rainfall estimation, *J. Hydrometeorol.*, 4, 43–61, 2003.
- Ulbrich, C. W.: Natural variations in the analytical form of the raindrop size distribution, *J. Clim. Appl. Meteorol.*, 22, 1764–1775, 1983.

## Characteristics of the raindrop distributions in RICO shallow cumulus

O. Geoffroy et al.

Title Page

Abstract

Introduction

Conclusions

References

Tables

Figures

⏪

⏩

◀

▶

Back

Close

Full Screen / Esc

Printer-friendly Version

Interactive Discussion



## Characteristics of the raindrop distributions in RICO shallow cumulus

O. Geoffroy et al.

Title Page

Abstract

Introduction

Conclusions

References

Tables

Figures



Back

Close

Full Screen / Esc

Printer-friendly Version

Interactive Discussion



- Ulbrich, C. W. and Atlas, D.: Rainfall microphysics and radar properties: analysis methods for drop size spectra, *J. Appl. Meteorol.*, 37, 912–923, 1998.
- van Zanten, M. C., Stevens, B., Vali, G., and Lenschow, D. H.: Observations of drizzle in nocturnal marine stratocumulus, *J. Atmos. Sci.*, 62, 88–106, 2005.
- 5 Waldvogel, A.: The  $N_0$  jump of raindrop spectra, *J. Atmos. Sci.*, 31, 1067–1078, 1974.
- Wood, R.: Drizzle in stratiform boundary layer clouds – Part 1: Vertical and horizontal structure, *J. Atmos. Sci.*, 62, 3011–3033, 2005.
- Yuter, S. E. and Houze, R. A.: Measurements of raindrop size distributions over the Pacific warm pool and implications for Z–R relations, *J. Appl. Meteorol.*, 36, 847–867, 1997.
- 10 Zhang, G., Vivekanandan, J., and Brandes, E.: A method for estimating rain rate and drop size distribution from polarimetric radar measurements, *IEEE T. Geosci. Remote*, 39, 830–841, 2001.

## Characteristics of the raindrop distributions in RICO shallow cumulus

O. Geoffroy et al.

**Table 1.** Values of  $v^*$ ,  $\sigma_g^*$ , the arithmetic mean  $v_{arith}$ ,  $\sigma_{arith}$ , and geometric mean  $v_{geom}$ ,  $\sigma_{geom}$  of the ensemble of shape parameter values. And values of  $v^*$  for spectra reconstructed using the Center-in (C) method, Entire-in method (E), spectra truncated above 1500  $\mu\text{m}$  (< 1500), under 300  $\mu\text{m}$  (> 300) and both (300–1500). All values are given for four resolutions: 1, 0.5, 0.2 and 0.05 Hz.

		1 Hz (~ 100 m)	0.5 Hz (~ 200 m)	0.2 Hz (~ 500 m)	0.05 Hz (~ 2000 m)
E2	$v^*$	3.2	2.7	2.2	1.6
E2	$\langle v \rangle_{geom}$	3.5	3.0	2.5	1.8
E2	$\langle v \rangle_{arith}$	6.7	5.5	4.4	3.2
E2	$\sigma_g^*$	1.63	1.67	1.72	1.81
E2	$\langle \sigma_g \rangle_{geom}$	1.59	1.63	1.68	1.76
E2	$\langle \sigma_g \rangle_{arith}$	1.62	1.66	1.71	1.79
E	$v^*$	2.4	1.9	1.5	1.0
C	$v^*$	2.2	1.8	1.3	0.9
E2 < 1500	$v^*$	3.3	2.8	2.3	1.8
E2 > 300	$v^*$	8.0	7.6	6.9	5.9
E2 300–1500	$v^*$	9.0	8.6	8.1	7.3

Title Page

Abstract

Introduction

Conclusions

References

Tables

Figures

⏪

⏩

◀

▶

Back

Close

Full Screen / Esc

Printer-friendly Version

Interactive Discussion

## Characteristics of the raindrop distributions in RICO shallow cumulus

O. Geoffroy et al.

**Table 2.** Values of the geometric mean  $\mu_{\log}$  and the geometric standard deviation  $\sigma_{\log}$  of the Log errors and the arithmetic mean  $\mu_{\text{abs}}$  and the arithmetic standard deviation  $\sigma_{\text{abs}}$  of the absolute errors of calculated for  $M_1$ ,  $M_2$ ,  $M_4$ ,  $M_6$ , for the Lognormal and the Gamma parametric functions, when using the constant trade-off tuning parameters values,  $\sigma_g^*$  and  $\nu^*$  and the parameterized value in function of  $N_r q_r$ ,  $\sigma_g^p$  and  $\nu^p$ .

	$M_1$	$M_2$	$M_5$	$M_6$
Lognormal, $\sigma_g^* = 1.63$			$\mu_{\log} \times \sigma_{\log}$	
	$1.08 \times 1.32$	$1.05 \pm 1.27$	$1.0 \pm 1.41$	$1.42 \pm 3.21$
			$\mu_{\text{abs}} \pm \sigma_{\text{abs}}$	
	$0.7 \pm 3.0$ ( $\mu\text{m cm}^{-3}$ )	$319 \pm 1232$ ( $\mu\text{m}^2 \text{cm}^{-3}$ )	$-2.4 \pm 16.8$ ( $10^8 \mu\text{m}^5 \text{cm}^{-3}$ )	$-4 \pm 184$ ( $10^{14} \mu\text{m}^6 \text{cm}^{-3}$ )
Gamma, $\nu_1^* = 3.2$			$\mu_{\log} \times \sigma_{\log}$	
	$1.06 \pm 1.32$	$1.06 \pm 1.27$	$0.93 \pm 1.41$	$0.87 \pm 3.21$
			$\mu_{\text{abs}} \pm \sigma_{\text{abs}}$	
	$0.7 \pm 2.9$ ( $\mu\text{m cm}^{-3}$ )	$328 \pm 1247$ ( $\mu\text{m}^2 \text{cm}^{-3}$ )	$-3 \pm 18$ ( $10^8 \mu\text{m}^5 \text{cm}^{-3}$ )	$19 \pm 184$ ( $10^{14} \mu\text{m}^6 \text{cm}^{-3}$ )
Lognormal, $\sigma_g^p$			$\mu_{\log} \times \sigma_{\log}$	
	$1.07 \times 1.27$	$1.05 \times 1.22$	$1.0 \times 1.32$	$1.38 \times 2.62$
			$\mu_{\text{abs}} \pm \sigma_{\text{abs}}$	
	$0.1 \pm 2.2$ ( $\mu\text{m cm}^{-3}$ )	$122 \pm 622$ ( $\mu\text{m}^2 \text{cm}^{-3}$ )	$0.3 \pm 8.4$ ( $10^8 \mu\text{m}^5 \text{cm}^{-3}$ )	$69 \pm 827$ ( $10^{14} \mu\text{m}^6 \text{cm}^{-3}$ )
Gamma, $\nu^p$			$\mu_{\log} \times \sigma_{\log}$	
	$1.02 \pm 1.26$	$1.04 \pm 1.22$	$0.95 \pm 1.32$	$0.91 \pm 2.55$
			$\mu_{\text{abs}} \pm \sigma_{\text{abs}}$	
	$-0.3 \pm 2.7$ ( $\mu\text{m cm}^{-3}$ )	$74 \pm 570$ ( $\mu\text{m}^2 \text{cm}^{-3}$ )	$1 \pm 9$ ( $10^8 \mu\text{m}^5 \text{cm}^{-3}$ )	$-1 \pm 122$ ( $10^{14} \mu\text{m}^6 \text{cm}^{-3}$ )

[Title Page](#)
[Abstract](#)
[Introduction](#)
[Conclusions](#)
[References](#)
[Tables](#)
[Figures](#)
[Back](#)
[Close](#)
[Full Screen / Esc](#)
[Printer-friendly Version](#)
[Interactive Discussion](#)


**Characteristics of the raindrop distributions in RICO shallow cumulus**

O. Geoffroy et al.

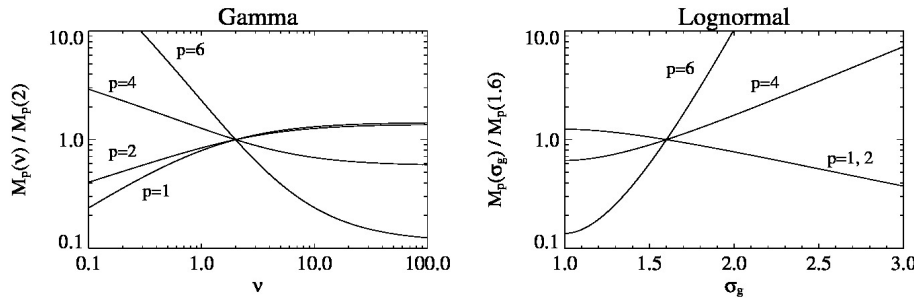


**Fig. 1.** Relationship between the moments of the order  $p = 1, 2, 4, 6$  and the shape parameter for the Gamma function (left) and the Lognormal function (right). Each moment is normalized by the value corresponding to  $\nu = 2$  for the Gamma function and  $\sigma_g = 1.6$  for the Lognormal function.

Title Page

Abstract Introduction

Conclusions References

Tables Figures

⏪ ⏩

⏴ ⏵

Back Close

Full Screen / Esc

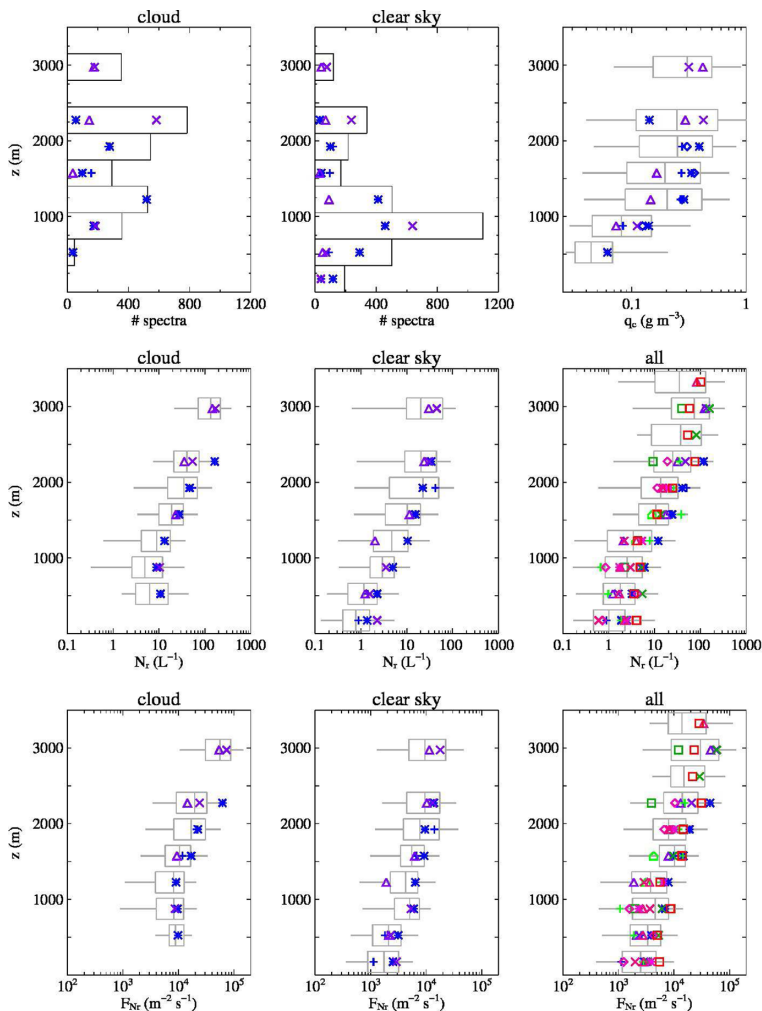
Printer-friendly Version

Interactive Discussion



**Characteristics of the  
raindrop distributions  
in RICO shallow  
cumulus**

O. Geoffroy et al.



Title Page

Abstract Introduction

Conclusions References

Tables Figures

◀ ▶

◀ ▶

Back Close

Full Screen / Esc

Printer-friendly Version

Interactive Discussion



**Fig. 2.** Total number of rain sampled spectra in cloud region (top row, left) and in clear sky (top row, right). The symbol denotes the contribution of each flight separately. Vertical profile of statistical distribution of cloud water content  $q_c$  (top, row right) sampled at 1 Hz for flights with Fast-FSSP measurements available (blue points) and vertical profile of statistical distribution of the rain variables sampled at 1 Hz for the rain concentration  $N_r$ , the rain concentration flux  $F_{Nr}$ , the rain water content  $q_r$ , the precipitation flux  $F_{qr}$  and the rain mean volume diameter  $D_v$ , in all regions (left), in the cloud region (middle) and in the clear sky region (right) (the last only for flights with Fast-FSSP available). The boxplots denote the 5th, 25th, 50th, 75th and 95th percentiles of the variable distribution in every 300 m layer. Symbols are mean values for each flight.

**Characteristics of the raindrop distributions in RICO shallow cumulus**

O. Geoffroy et al.

<a href="#">Title Page</a>	
<a href="#">Abstract</a>	<a href="#">Introduction</a>
<a href="#">Conclusions</a>	<a href="#">References</a>
<a href="#">Tables</a>	<a href="#">Figures</a>
<a href="#">⏪</a>	<a href="#">⏩</a>
<a href="#">◀</a>	<a href="#">▶</a>
<a href="#">Back</a>	<a href="#">Close</a>
<a href="#">Full Screen / Esc</a>	
<a href="#">Printer-friendly Version</a>	
<a href="#">Interactive Discussion</a>	



**Characteristics of the  
raindrop distributions  
in RICO shallow  
cumulus**

O. Geoffroy et al.

Title Page

Abstract

Introduction

Conclusions

References

Tables

Figures

◀

▶

◀

▶

Back

Close

Full Screen / Esc

Printer-friendly Version

Interactive Discussion

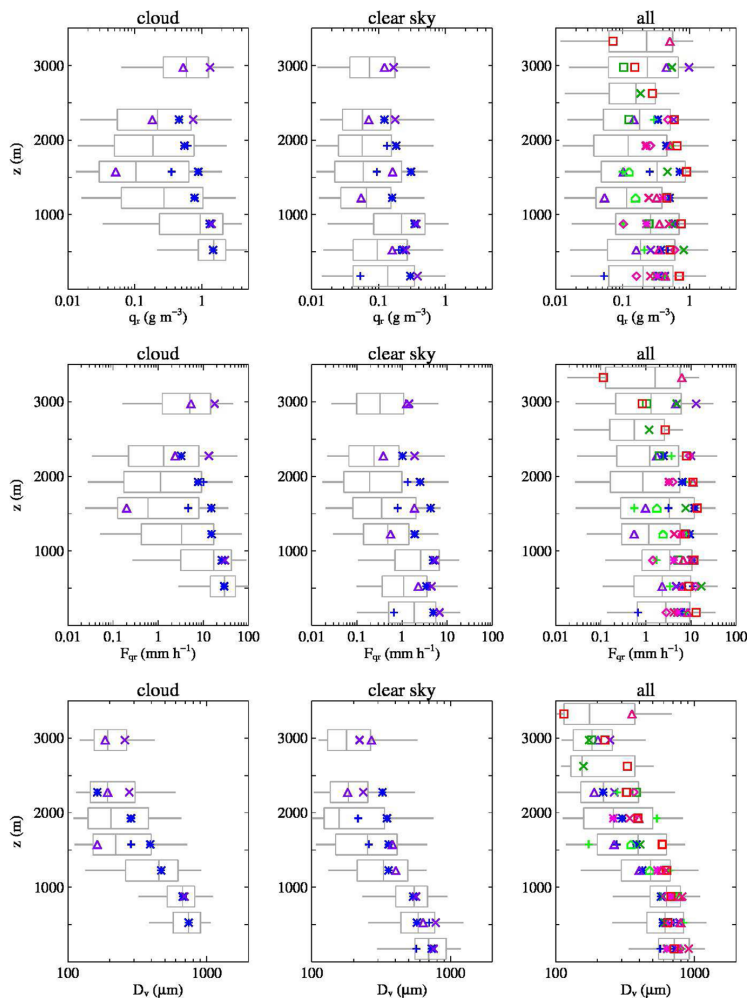
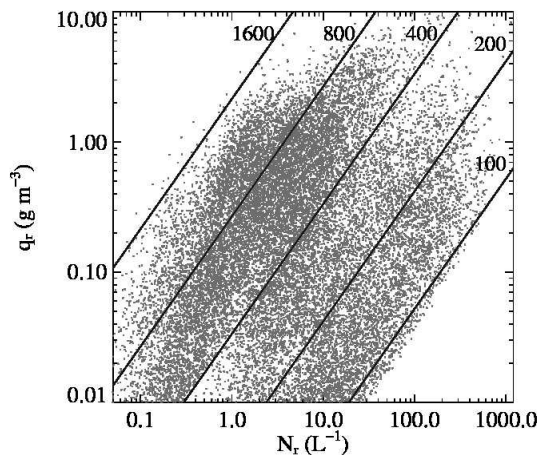


Fig. 2. Continued.

## Characteristics of the raindrop distributions in RICO shallow cumulus

O. Geoffroy et al.



**Fig. 3.** Scatter-plot of the drop number concentration,  $N_r$ , and the rain water content,  $q_r$ , for drop spectra sampled at 1 Hz. Lines represent constant mean volume diameters for  $D_v = 1600, 800, 400, 200, 100 \mu\text{m}$ .

[Title Page](#)[Abstract](#)[Introduction](#)[Conclusions](#)[References](#)[Tables](#)[Figures](#)[⏪](#)[⏩](#)[⏴](#)[⏵](#)[Back](#)[Close](#)[Full Screen / Esc](#)[Printer-friendly Version](#)[Interactive Discussion](#)

## Characteristics of the raindrop distributions in RICO shallow cumulus

O. Geoffroy et al.

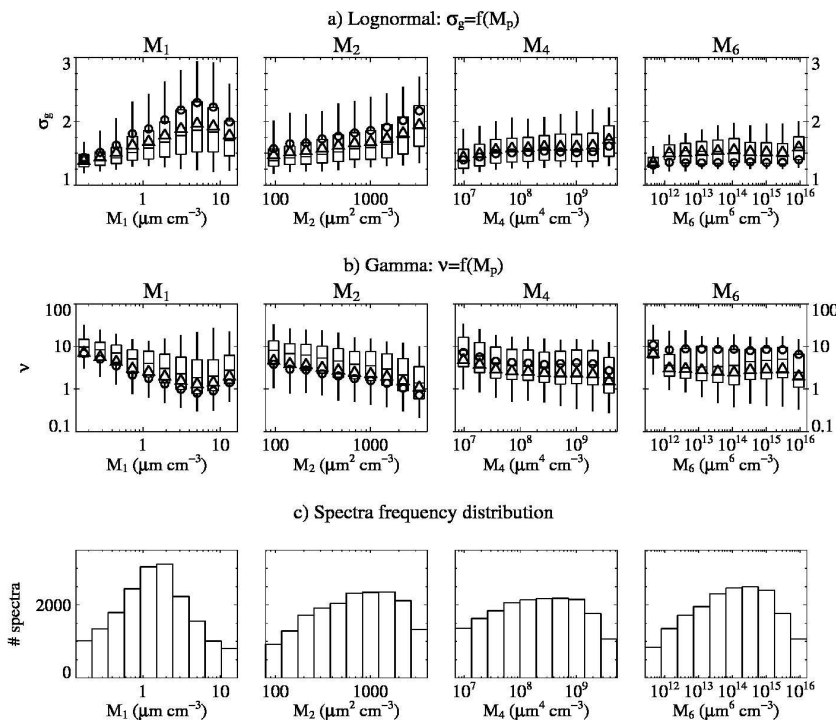


**Fig. 4.** Statistical distribution of the shape parameter values as a function, from left to right, of the  $M_1$ ,  $M_2$ ,  $M_4$ , and  $M_6$  moment values. The  $x$  axis is divided into 10 classes on a Logscale. The boxplots denote the 5th, 25th, 50th, 75th and 95th percentiles of the shape parameter distribution in each class. The circles and triangles denote the tuning parameter value that minimizes the standard deviation of the absolute error and the geometric standard deviation of the Log error in each class, respectively. The top and second rows are for the Lognormal function and the Gamma function, respectively. The third row shows the number of sampled spectra in each moment class.

## Characteristics of the raindrop distributions in RICO shallow cumulus

O. Geoffroy et al.

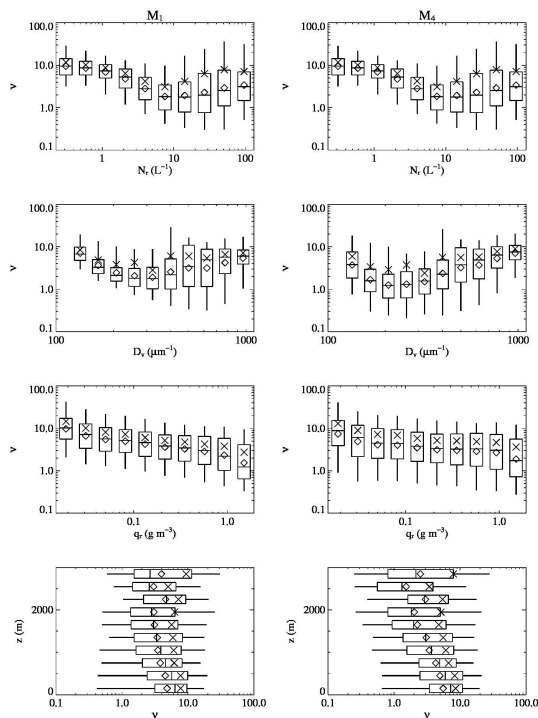


**Fig. 5.** Statistical distribution of the shape parameter values as a function of rain number concentration  $N_r$  (upper line), rain mean volume diameter  $D_v$  (2nd line) and rainwater content (3rd line) and profile of the statistical distribution of the shape parameter values (lower line) for the  $M_1$  minimization (left row) and the  $M_4$  minimization (right row). The boxplots denote the 5th, 25th, 50th, 75th and 95th percentiles of the shape parameter distribution in each class. The diamonds and crosses denote the arithmetic mean and the geometric mean in each class, respectively.

[Title Page](#)
[Abstract](#)
[Introduction](#)
[Conclusions](#)
[References](#)
[Tables](#)
[Figures](#)
[◀](#)
[▶](#)
[◀](#)
[▶](#)
[Back](#)
[Close](#)
[Full Screen / Esc](#)
[Printer-friendly Version](#)
[Interactive Discussion](#)

**Characteristics of the  
raindrop distributions  
in RICO shallow  
cumulus**

O. Geoffroy et al.

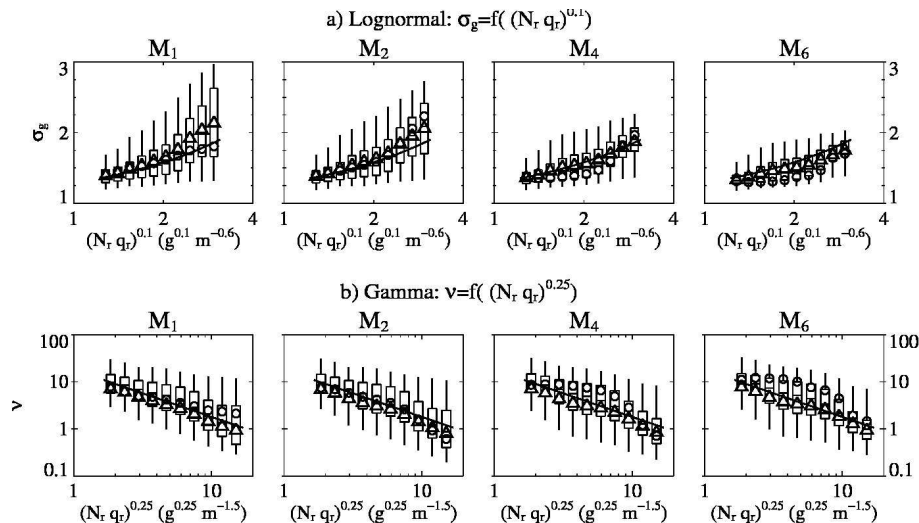


**Fig. 6.** Same as Fig. 4 but plotted as a function of a power law of  $q_r N_r$ . The thick lines represent the proposed parameterizations for the variable shape parameter.

Title Page

Abstract Introduction

Conclusions References

Tables Figures

◀ ▶

◀ ▶

Back Close

Full Screen / Esc

Printer-friendly Version

Interactive Discussion

